SCIENTIFIC REPORTS

OPEN

SUBJECT AREAS:
SOFT MATERIALS
BIOMEDICAL MATERIALS
BIOMATERIALS
NANOMEDICINE

Received
24 May 2013

Accepted
18 July 2013

Published
5 August 2013

Correspondence and requests for materials should be addressed to Z.F.D. (zhifei.dai@pku.edu.cn)

Polypyrrole Hollow Microspheres as Echogenic Photothermal Agent for Ultrasound Imaging Guided Tumor Ablation

Zhengbao Zha[2], Jinrui Wang[1], Enze Qu[1], Shuhai Zhang[2], Yushen Jin[2], Shumin Wang[1] & Zhifei Dai[1]

[1]College of Engineering and Peking University Third Hospital, Peking University, Beijing 100871, China, [2]School of Life Science and Technology, Harbin Institute of Technology, Harbin 150080, China.

Ultrasound (US) imaging provides a valuable opportunity to administer photothermal therapy (PTT) of cancer with real-time guidance to ensure proper targeting, but only a few theranostic agents were developed by physically grafting near infrared (NIR)-absorbing inorganic nanomaterials to ready-made ultrasound contrast agents (UCAs) for US imaging guided PTT. In this paper, NIR absorbing hollow microspheres were generated from polypyrrole merely using a facile one-step microemulsion method. It was found that the obtained polypyrrole hollow microspheres (PPyHMs) can act as an efficient theranostic agent not only to enhance US imaging greatly, but also exhibit excellent photohyperthermic effects. The contrast consistently sustained the echo signals for no less than 5 min and the NIR laser light ablated the tumor completely within two weeks in the presence of PPyHMs. More importantly, no use of additional NIR absorber substantially minimizes an onetime dose of the theranostic agent.

Photothermal therapy (PTT) has gained popularity recently as a promising minimally invasive alternative to conventional surgery and chemotherapy[1–3]. With the support of photothermal agents which exhibit strong absorption in the tissue transparent near-infrared (NIR) region (700 ~ 1100 nm), PTT could effectively ablate tumor cells by delivering a specific amount of photoenergy directly into tumor tissues without systemic effects[2]. However, for effective and safe PTT treatment, real-time imaging of *in vivo* photothemral agents delivery, distribution and monitoring of post-treatment therapeutic outcomes with appropriate imaging techniques are crucial to design and optimize personalized PTT treatment[4–6]. Therefore, upgrading photothermal agents to theranostic agents by integrating imaging capability has received increased attention owing to the requirement of sufficient agent accumulation in diseased areas both for imaging and therapy[7].

Ultrasound (US) imaging provides a valuable opportunity to administer anticancer therapy with real-time guidance to ensure proper targeting. Because of its readily availability for portable devices, low cost, and lack of radiation exposure[8–11], percutaneous US has become a favorite tool to target cancer. Moreover, endoscopic ultrasound (EUS) guided therapy has emerged as a promising and rapidly developing field that adds another dimension to US-guided therapy[12]. Uniquely, EUS can direct therapy toward intraabdominal cancers that can be difficult to access by percutaneous routes. Furthermore, it has been demonstrated as a powerful technique to estimate the temperature change during PTT by measuring thermally induced differential motion of speckle[13,14]. Despite the significant advantages of US imaging for guiding PTT, only a few theranostic photothermal agents with capability to enhance US imaging were developed by physically grafting NIR-absorbing Au-nanoshell[15], Au nanorods[16] or CuS nanoparticles (NPs)[17] to ready-made ultrasound contrast agents (UCAs) which are usually microbubbles. Nevertheless, such type of hybrid theranostic agents still encountered numerous obstacles since the incorporating inorganic components would affect the UCAs acoustic response, i.e., a change in the shell stiffness results in the change of the acoustic spectrum and resonance frequency of UCAs. In particular, microbubble echogenic response at a certain frequency may be reduced. In addition, the potential long-term toxicity of the added inorganic components would hinder their further *in vivo* applications[18–20]. The simple physical combination of different diagnostic and therapeutic element would give a relatively high onetime dose which may cause systemic toxicity and impose an extra burden for the patients to excrete the theranostic agents[21,22]. Attacking these

problems head on, the development of photothermal agents with excellent echogenic response merely from biocompatible organic components is highly pursued.

Polypyrrole (PPy) materials have received great attention in bioelectronics and biomedical application due to their inherent features, including high conductivity, outstanding stability and good biocompatibility[23–25]. Encouraged by the *in vivo* animal studies that low concentrations of PPy NPs (<200 μg mL^{-1}) have very low long-term cytotoxicity[26], PPy NPs have been demonstrated as an attractive OCT-absorbing (optical coherence tomography) contrast agent for tumor imaging[27] and photothermal agent with high photothermal conversion efficiency for tumor ablation[28] owing to the strong NIR absorption spectrum. Due to the truth that typical UCA is based upon microscale bubbles which are effective scatters of ultrasound waves[29], it is highly desired to develop biocompatible NIR-absorbing PPy hollow microspheres (PPyHMs) with outstanding US-responsive capability for US imaging guided PTT. However, due to the inferior solubility of polypyrrole materials in common solvents[30], PPyHMs in previous studies were commonly fabricated from in situ polymerization of pyrrole monomer on sacrificial templates, such as polystyren microspheres[29]. The complicatd fabrication process and poor dispersity of PPyHMs hindered their further biomedical applications.

Herein, a photothermal UCA was first time constructed merely from polypyrrole *via* a facile oil-in-water (O/W) microemulsion method (Fig. 1a). Polypyrrole was employed as both NIR photoabsorber and membrane materials for UCA construction. Thus, the obtained PPyHMs can act as an efficient theranostic agent not only to enhance ultrasound imaging greatly, but also exhibit excellent photohyperthermic effect for ablation of tumors due to their strong absorption of polypyrrole in the near-infrared region. More importantly, no additional inorganic NIR absorber or contrast agent materials was used in this echogenic photothermal agent of PPyHMs, substantially minimizing an onetime dose and lowering an extra burden for the patients to excrete the theranostic agents.

Results

Preparation and characterization of water-dispersible PpyHMs. For the fabrication of water-dispersible PPyHMs, pyrrole monomer was first polymerized *via* a facile chemical oxidation with functional doping agent of di(2-ethylhexyl) sulfosuccinate sodium salt (NaDEHS), resulting in the soluble PPy complex ($[(Py)_3^+(DEHS)^-]_x$) (Fig. S1)[30,31]. The molecular weight of the obtained $[(Py)_3^+(DEHS)^-]_x$ was determined to be 71933.7 (Fourier Transform Mass Spectroscopy, Bruker Solarix FTMS) (Fig. S2). Assuming a repeat unit of composition $(Py)_3^+(DEHS)^-$ (Mw = 616.80), there are 116 units of $(Py)_3^+(DEHS)^-$ per polymer chain, *i.e.* 348 pyrrole units per polymer chain. Then, PPyHMs were generated by the O/W microemulsion method using $[(Py)_3^+(DEHS)^-]_{116}$ with polyvinylpyrrolidone (PVP) as a stabilizer.

The typical morphology of the PPyHMs was analyzed by scanning electron microscopy (SEM) and transmission electron microscopy (TEM). The PPyHMs showed a well-defined spherical shape and the diameter range from hundreds of nanometers to several micrometers with an average of about 0.876 μm. The hollow structure of PPyHMs is confirmed by some broken and collapsed PPyHMs during the lyophilisation process with PVP as a stabilizer by SEM observation, further evidenced by ultrathin section TEM characterization of PPyHMs (Fig. 1b). In contrast, no broken and collapsed PPy microspheres were obtained when polyvinyl alcohol (PVA) was used as a stabilizer (Fig. 1c). As shown in Fig. S3, PPyHMs showed a broad absorption band extending from the visible to the NIR region in water, which endows the potential application of PPyHMs for NIR light induced PTT. The absorbance increased linearly as elevating the concentration of PPyHMs in water, suggesting the good dispersibility of PPyHMs in aqueous solution. Furthermore, no macroscopic aggregates were observed when PPyHMs were dispersed in RPMI-1640 culture medium with a zeta-potential of around −5.2 mV, indicating the good colloidal stability. It was further evidenced by the linearly increased absorbance with increased PPyHMs concentrations (Fig. 1d). Thus, an obvious concentration-dependent temperature increase was observed for PPyHMs solutions under laser irradiation (Fig. 1e). In particular, the solution temperature was elevated from 19.5°C to 50.6°C when 100 μg mL^{-1} PPyHMs solution exposed to NIR laser for 10 min while only 1.1°C temperature elevation occurred in the absence of PPyHMs, confirming that PPyHMs could act as an efficient photothermal agent.

Ultrasound imaging of PPyHMs. To explore the applications of PPyHMs in biomedicine, their diagnostic potential as an ultrasound contrast agent was first evaluated both *in vitro* and *in vivo*. According to our previously described procedure[15], a suspension of PPyHMs was injected into a latex tube containing circulating saline. As shown from Fig. 2a and 2b, when the concentration of PPyHMs solution was ranged from 0 mg mL^{-1} to 25 mg mL^{-1}, the generated US signals increased proportionally at low concentrations while the echo intensity was almost saturated at 10 mg mL^{-1}. Moreover, the *in vitro* echo stability test showed that PPyHMs were persisted not fewer than 5 min with an 86% persistence of US signal intensity under sustained ultrasound irradiation (Fig. 2c). A further evaluation of the ultrasound contrast behaviour of PPyHMs was carried out *in vivo* using New Zealand white rabbits. Ultrasound contrast images with and without agent injection in both pulse-inversed harmonic imaging (PIHI) mode and conventional B mode are shown in Fig. 2d, 2e. Excellent enhancements of rabbit kidney images were clearly seen in a few seconds after bolus intravenous injection of the agent (Fig. 2e), indicating that PPyHMs were able to traverse pulmonary capillaries to achieve systemic enhancement and is consistent with the results of *in vitro* ultrasonography. More interestingly, the contrast consistently sustained the echo signals for no less than 5 min. On the contrary, in the case of Sonovue®, the echo signals transiently persisted and the half-life of the echo signals occurred within 2 ~ 3 min, as expected. The vital signs of the rabbits were unaffected during the entire procedure, and no arrhythmia and other side effects were observed, demonstrating no acute toxicity of PPyHMs.

Localized photohyperthermic effect. The ideal photothermal agents should be non-toxic or low-toxic for biomedical applications. To quantitatively evaluate the cytotoxicity of PPyHMs, a standard methyl thiazolyl tetrazolium (MTT) assay with the Human Umbilical Vein Endothelial Cells (HUVECs) was used. It was found that the as-prepared PPyHMs appear to be largely biocompatible, the percentage of viable cells for HUVECs was 81.7 ± 1.9% after 24 hrs exposure to PPyHMs with a concentration of as high as 300 μg mL^{-1} (Fig. 3g). Next, PPyHMs were used as the photothermal agent for *in vitro* cancer cell ablation under laser irradiation. U87-MG cells (human glioblastoma cell lines) were incubated with 80 μg mL^{-1} PPyHMs suspended with DMEM culture medium, followed by irradiation with a NIR laser (808 nm and 6 W cm^{-2} for 0 min, 3 min, 5 min and 10 min). Then, the cells were co-stained with calcein AM and propidium iodide (PI) to differentiate live (green) and dead (red) cells, respectively. No apparent change in cell viability and density was observed when cells treated with laser or PPyHMs alone compared with the negative control without laser and PPyHMs (Fig. 3a, 3b and 3c). In comparison, U87-MG cells treated with PPyHMs plus a NIR laser experienced substantial cellular death, and the cell death area expanded as NIR light irradiation time increased (Fig. 3d, 3e and 3f).

Further quantitative evaluation on U87-MG cell viabilities after PTT treatment indicated that the photo-cytotoxicity of PPyHMs was in both dose-dependent and irradiation time-dependent manner (Fig. 3h). PPyHMs showed almost no toxicity to U87-MG cells without NIR light illumination. In contrast, when simultaneously treated

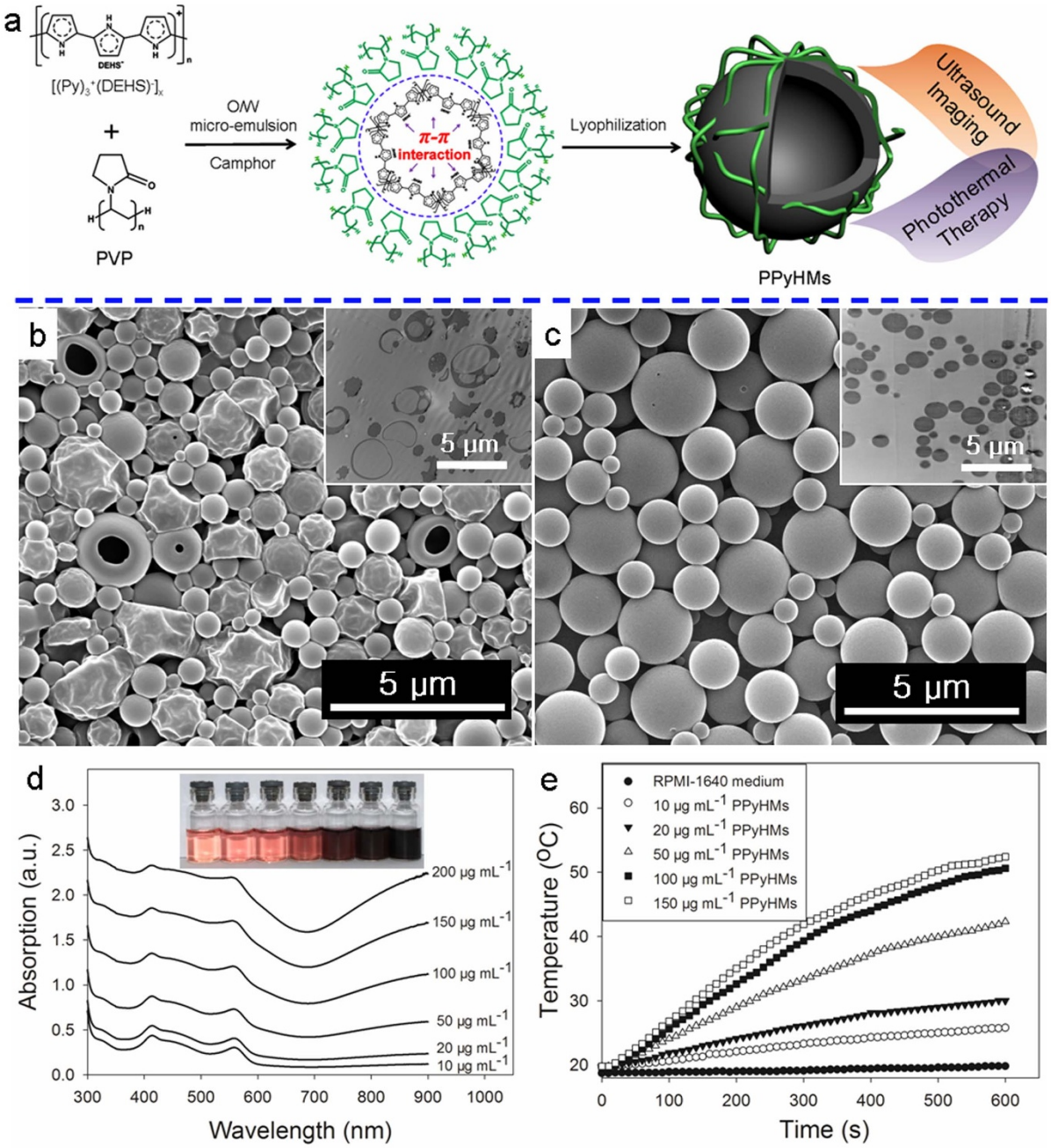

Figure 1 | Preparation and characterization of water-dispersible PPyHMs. (a) Schematic illustration of the formation of echogenic PPyHMs for combined US imaging and PTT via a facile O/W microemulsion method; SEM and ultrathin-section TEM images of obtained PPyHMs with (b) PVP and (c) PVA as stabilizers; (d) UV-vis-NIR spectra of various concentrations PPyHMs dispersed in RPMI-1640 culture medium, inset was the photograph for various concentrations of PPyHMs dispersed in RPMI-1640 culture medium, indicating good dispersibility; (e) Heating curves of PPyHMs in RPMI-1640 culture medium at different concentrations under 808 nm laser irradiation.

with PPyHMs and NIR laser illumination (808 nm, 6 W cm^{-2}, 5 min), the cell viabilities significantly decreased as the concentration increased. Only less than 20% of cells remained viable when they were incubated with 7 μg mL^{-1} or higher concentration of PPyHMs under NIR laser irradiation, thus indicating a significant photothermal therapeutic effect for U87-MG cells. Moreover, enhanced cytotoxicity was observed with increased irradiation time. At a concentration of 7 μg mL^{-1} of PPyHMs, the cell viabilities of U87-MG cells were 106.4 ± 10.9%, 56.2 ± 2.4% and 13.7 ± 2.5% with different NIR light illumination time of 0 min, 3 min and 5 min, respectively. These experimental findings demonstrated that the PPyHMs could act as an effective NIR photoabsorber to localizedly kill the tumor cells *in vitro*.

***In vivo* US imaging guided PTT.** Encouraged by the effective PPyHMs-induced photothermal ablation of cancer cell *in vitro*, a further *in vivo* US imaging guided PTT was studied using PPyHMs as the photothermal agent in a U87-MG tumor mouse model. Female Balb/c nude mice bearing U87-MG tumors were divided into 4 groups with 8 mice in each group: control group, laser-only group, PPyHMs-only group and PPyHMs + laser group. PPyHMs (200 μL, 2 mg mL^{-1} suspension in saline) were intratumorally injected into the mice of PPyHMs-only and PPyHMs + laser groups, while saline (200 μL) in control and laser-only groups, respectively. During the injection of the PPyHMs, tumor areas of PPyHMs + laser groups were displayed *via* US contrast imaging to ensure the evenly distribution of the agent and guide the following PTT (Fig. 4b).

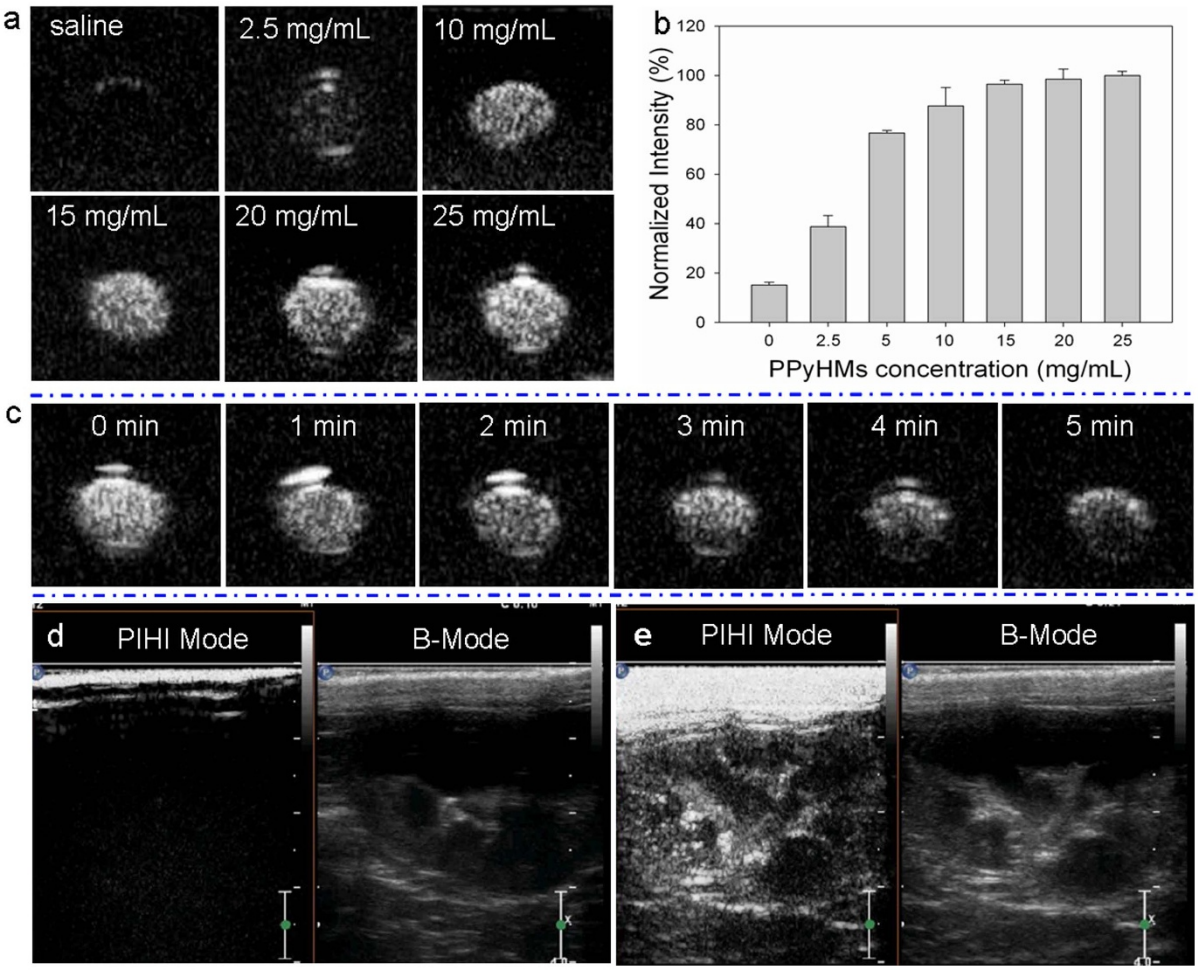

Figure 2 | Ultrasound imaging of PPyHMs. *In vitro* ultrasound contrast-enhanced images in a latex tube (a) US images of various concentrations of PPyHMs; (b) Normalized US intensities over PPyHMs concentration; (c) Time-dependent echogenic behaviors of PPyHMs at the concentration of 20 mg mL^{-1}. *In vivo* ultrasonograms in the rabbit right kidney (d) pre- and (e) post-administration of PPyHMs.

Then the tumor-bearing mice of laser-only and PPyHMs + laser groups with continuous anesthesia were exposure to the 808 nm laser with a low power density of 0.64 W cm^{-2}. The local temperature change was monitored by an infrared (IR) thermal camera (Fig. 4a). The plot of average temperature in the tumor areas of mice from PPyHMs + laser group could rapidly increased to ~60°C within 5 min, which was high enough to kill tumor *in vivo*. In marked contrast, the temperature of the tumor without PPyHMs injection was not obviously affected even after being exposed to the laser irradiation, showing only 5°C temperature increase within 10 min (Fig. S4).

The therapeutic effectiveness was evaluated with the tumor volume variation. It was found that the tumors were effectively ablated only after PPyHMs injection and laser exposure, leaving black scars at their original sites without showing reoccurrence. Unlike the PPyHMs + laser group, tumors in other three control groups showed similar growth speed, suggesting that either laser irradiation at this power density (0.64 W cm^{-2}) or PPyHMs alone does not affect the tumor development (Fig. 4c, d). Further haematoxylin and eosin (H&E) staining of tumor slices was carried out for tumors collected immediately after laser irradiation (Fig. 4e). As expected, significant cancer cell damage, such as karyorrhexis and karyolysis, was noticed only in the tumor with both PPyHMs injection and laser irradiation, but not in other three control groups, confirming again the excellent therapeutic effectiveness of PPyHMs under NIR laser irradiation. It should be pointed that we used a rather low laser power density (0.64 W cm^{-2}) to minimize the adverse effects, indicating excellent photothermal conversion efficiency of PPy materials as previously reported[28].

Body weight (subtract tumor weight) loss was used as a measure of treatment induced toxicity. As shown in Fig. S5, no significant difference was observed in each group after treatment for 14 days, demonstrating that all treatments were tolerated well by the tumor-bearing animals and the photothermal treatment showed no unacceptable toxicity. The vital organs of mice bearing U87-MG tumors after PTT treatment were collected for further histological examination (n = 5) with a control group of age-matched healthy mice. Neither noticeable organ damage nor inflammation was observed compared with the control group (Fig. S6), indicating the PPyHMs based *in vivo* photothermal treatment of cancer induced no significant side effect to the treated mice.

Discussion

PPy materials have drawn tremendous interests of researchers in bioelectronics and biomedical application due to their inherent features, including high conductivity, outstanding stability and good biocompatibility[32]. However, one of the obstacles for their practical applications was their poor solubility in common solvents due to the strong interactions between the polymer chains[30]. In order to solve this problem, various methods have been reported to prepare soluble PPy by chemical modification such as attachment of a functional group to β-carbon and/or nitrogen positions of the pyrrole unit[33]. Another strategy to obtain high solubility is to dope the polymer with anionic surfactant which enhances the solubility by promoting the

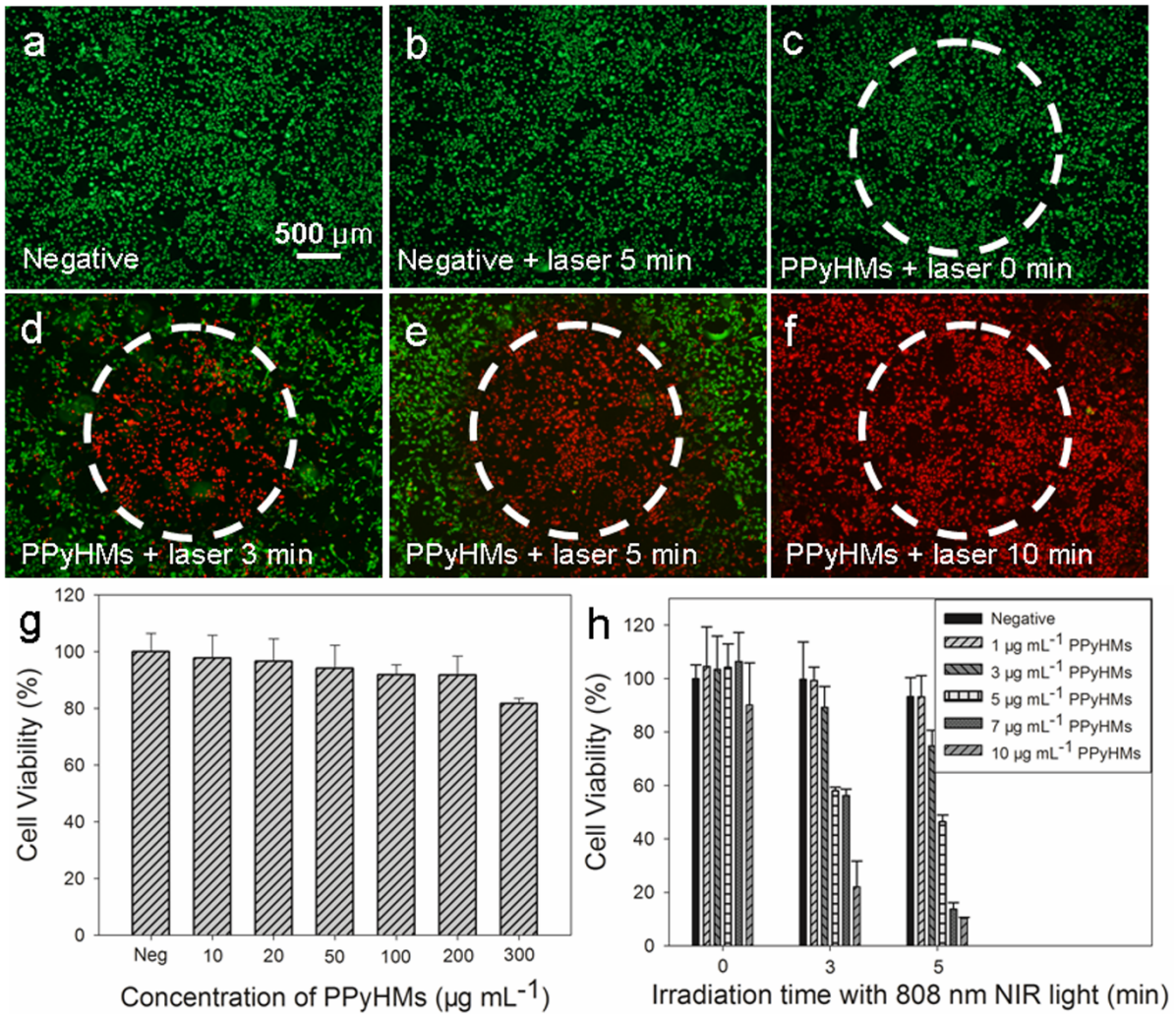

Figure 3 | **Localized photohyperthermic effect.** Photothermal destruction of U87-MG cells with or without PPyHMs and NIR laser (808 nm, 6 W cm^{-2}) treatments (a, b, c, d, e and f). White circle indicates the laser spot; live/dead stain for viability shows dead cells as red while viable cells as green; (g) Cell viability of HUVECs with 24 h exposure to various concentrations of PPyHMs; (f) U87-MG cell viability after treatment with different concentrations of PPyHMs and NIR laser for different irradiation time.

compatibility between PPy chain and the solvent. Unlike the chemical modification method, this approach does not alter the chemical structure of PPy itself but affects the charge on the polymer backbone depending upon the doping level[30].

In our study, the soluble PPy complex ($[(Py)_3^+(DEHS)^-]_{116}$) was synthesized *via* a facile chemical oxidation of pyrrole monomer with functional doping agent of NaDEHS. And then PPyHMs with good dispersity in aqueous solution were first time developed as an photothermal agent with US-responsive capability *via* a facile O/W microemulsion method. Due to the π–π stacking interaction between $[(Py)_3^+(DEHS)^-]_{116}$ and PVP molecules, the $[(Py)_3^+(DEHS)^-]_{116}$ molecules tend to gather at the oil-water interface and then PPyHMs were formed after lyophilization. As evidenced by SEM and TEM characterization, PPyHMs with hollow interior were only obtained when PVP molecules were used as stabilizers while solid PPy microspheres were formed with PVA stabilizer, confirming the existent π–π stacking interaction between soluble $[(Py)_3^+(DEHS)^-]_{116}$ and PVP molecules again. Furthermore, a key criterion for the use of PPyHMs in biomedical application is the ability to maintain the colloidal stability in body to prevent a blockage of the blood vessels or being eliminated by the body's reticuloendothelial system (RES)[34]. As shown in Fig. 1d, the good dispersibility of PPyHMs in RPMI-1640 culture medium is due to the strong hydrophilicity of PPyHMs functionalized with PVP, which could suppress non-specific protein adsorption.

Due to the hollow structure of PPyHMs, we checked the US-responsive properties of PPyHMs both *in vitro* and *in vivo*. Excellent enhancements of tube *in vitro* and rabbit kidney images *in vivo* suggested the good contrast-enhancing ability of as-prepared PPyHMs. Benefiting from the high NIR absorbance, PPyHMs could serve as efficient photoabsorbers for NIR photothermal tumor ablation both *in vitro* and *in vivo*. Particularly, only less than 20% of U87-MG cells remained viable when they were incubated with 7 μg mL^{-1} or higher concentration of PPyHM under NIR laser irradiation. Moreover, no noticeable *in vitro* or *in vivo* side effects of PPyHM has been observed yet at our tested doses.

In summary, we have successfully constructed PPyHMs with high dispersibility and good stability from a facile one-step microemulsiom method using an efficient NIR photoabsorber of PPy complex. The PPyHMs not only provided excellent contrast enhancement for ultrasound imaging, but also ablated tumor efficiently upon NIR light irradiation. Combining US imaging and PTT through PPyHMs is especially attractive for reasons of low dose, simplicity and cost-effectiveness. Moreover, no need to incorporate additional NIR absorbing inorganic components into UCAs can avoid changing the shell stiffness which may result in the change of the acoustic

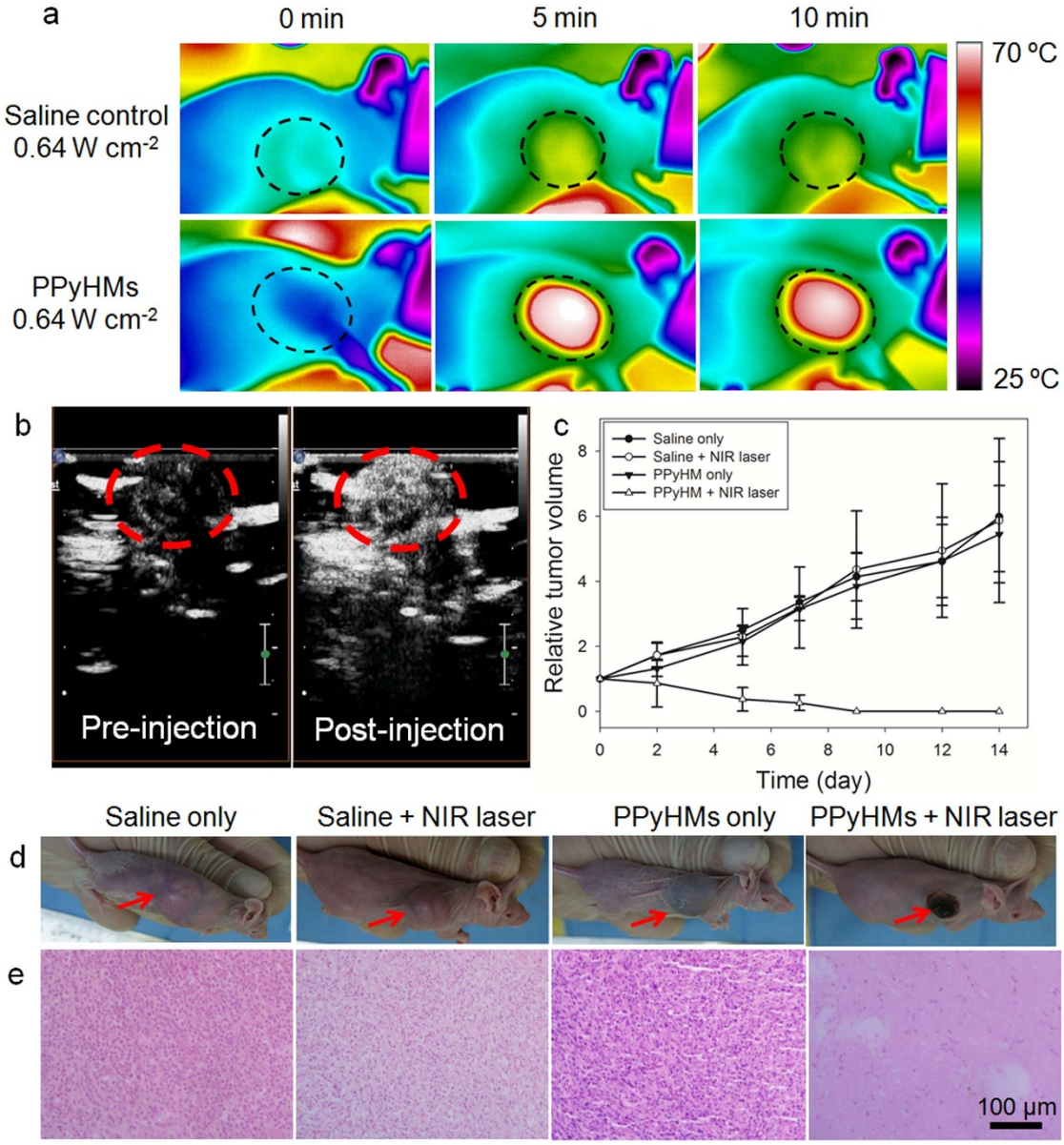

Figure 4 | ***In vivo*** **US imaging guided photothermal therapy.** (a) IR thermal images of tumor-bearing mice with and without PPyHMs injection exposed to the NIR laser at the power density of 0.64 W cm^{-2} recorded at different time intervals. (b) contrast-enhanced ultrasonograms after the intratumoral injection of PPyHMs (0.2 mL, 2 mg mL^{-1}) into the mice from PPyHMs + laser group for visualization of the agent distribution to guide the following PTT (tumors are highlighted in the red circles). (c) The tumor growth curves of different groups of mice after PTT treatment. The tumor volumes were normalized to their initial sizes. (d) Representative photographs of mice bearing U87-MG tumors after various different treatments indicated. (e) H&E stained tumor slices collected from different groups of mice immediately after laser irradiation. The PPyHMs injected tumor was severely damaged after laser irradiation.

spectrum and resonance frequency of UCAs. By utilization of enhancing ultrasound imaging and promoting photothermal effect, PPyHMs can be used as a theranostic agent to identify the size and location of the tumor, and then, under real-time ultrasound guidance and monitoring, NIR laser-induced photothermal therapy could be targetedly carried out. Therefore, PPyHMs have great potential as a new generation of theranostic agent for clinical applications.

Methods

Materials. Pyrrole (98%, Aldrich), sodium di(2-ethylhexyl) sulfosuccinate (NaDEHS, Aladdin Chemistry Co. Ltd.), Ammonium peroxydisulfate (APS, Aladdin Chemistry Co. Ltd.), polyvinylpyrrolidone (PVP, ~30 kDa, Sigma-Aldrich) and camphor (Sigma-Aldrich) were all used as received without further purification. De-ionized water (DI water, 18.2 MΩ•cm) from Milli-Q Gradient System was used in all the preparation.

Synthesis of soluble polypyrrole complex. Pyrrole (0.4 mol) and NaDEHS (0.15 mol) were mixed in DI water (900 mL in a 1 L beaker) with magnetic stirring and cooled to 0°C. APS (0.1 mol) dissolved in 100 mL DI water, was cooled to 0°C and added during ~2 min with magnetic stirring to the pyrrole/NaDEHS solution. The reaction mixture was held at 0°C for 20 h with magnetic stirring. The precipitate of doped polypyrrole $[(Py)_3^+(DEHS)^-]_{116}$, was obtained after centrifugation and washing with DI water and dried in vacuum for further use.

Fabrication of water-dispersible PPyHMs via a facile O/W micro-emulsion method. $[(Py)_3^+(DEHS)^-]_{116}$ (100 mg) and camphor (300 mg) was dissolved in methylene chloride (4.0 mL). Then the O/W microemulsion was generated by adding the oil phase of $(Py)_3^+(DEHS)^-]_x$ to the PVP aqueous solution (2% w/v, 20 mL), allowed for continuous homogenizing for 2 min. After magnetic stirring for 2 h, the microspheres were collected by three centrifugation (5000 g, 5 min, Avanti J-25, Beckman Coulter)/washing cycles. Followed by lyophilisation using a freeze dryer (TFD5505, IIshin Lab, Korea) for 2 days, the PPyHMs were obtained.

Acoustic imaging. *In vitro* ultrasonography of PPyHMs was carried out in the latex tube (with the inner diameter of ~5 mm) using a broadband linear array L9-3 transducer (9 to 3 MHz extended) of IU22 ultrasound system (Philips Medical Systems). The PPyHMs were dispersed in 0.9% saline at the concentration of 5 mg mL^{-1} and injected to the latex tube stimulating the blood vessel and both PIHI mode and conventional B-mode at the same time from the longitudinal cross section of the tube. For *in vivo* study, three rabbits (average weight of 2.5 kg) were anesthetized with pentobarbital sodium (2.0 mL per kg weight, 2% w/v in 0.9% saline) administration through ear vein, and subsequently, heparin sodium (4.0 mL, 0.2% w/v in 0.9% saline) was injected to avoid coagulation. The animals were placed on a warm blanket to keep body temperature within normal range during the experiment. The PPyHMs suspension (40 mg mL^{-1} in 0.9% saline) was intravenously injected at a concentraion of 0.1 mL per kg weight through a catheter, flushed with saline (1.0 mL) thereafter. The kidney was imaged transabdominally using a broadband L9-3 transducer in PIHI mode and conventional B-mode. All the digital clips and images were stored for off-line review. All the animal experiments were approved by the Institutional Animal Care and Use Committee of Peking University and carried out ethically and humanely.

Cell culture. HUVECs and U87-MG cells were cultured in standard cell media recommended by American type culture collection (ATCC). HUVECs seeded into 96-well plates were incubated with different concentrations of PPyHMs for 24 h. Relative cell viabilities were determined by the standard MTT assay. For *in vitro* PTT, U87-MG cells were incubated with and without different concentrations of PPyHMs and then irradiated by an 808 nm laser at a power density of 6 W cm^{-2} for different time. The cells were stained with Calcein AM/PI for qualitative and MTT assay for quantitative evaluation of the photo-toxicity.

Animal experiments. Femal Balb/c mice, female, 6 ~ 8 weeks, weigh approximately 18 ~ 22 g, were purchased for the study from Peking University Health Science Center of Laboratory Animal Science (PUHSCLAS, Beijing, China). All the animal experiments were approved by the Institutional Animal Care and Use Committee of Peking University and carried out ethically and humanely. 3×10^6 U87-MG cells suspended in 100 μL phosphate buffered saline (PBS) were subcutaneously injected into the right front flank of each female Balb/c mouse. The treatment started when the tumor size reaches approximately 300 mm^3.

Photothermal therapy *in vivo*. Mice bearing U87-MG tumors were intratumorally injected with 200 μL of 2 mg mL^{-1} PPyHMs. For control groups, mice were treated with the same volume of saline. Mice with and without PPyHMs injection were irradiated with the 808 nm NIR laser at a power density of 0.64 W cm^{-2} for 10 min. The tumor sizes were measured by a caliper every other day and calculated as the volume = (tumor length) × (tumor width)^2/2. Relative tumor volumes were calculated as V/V_0 (V_0 is the tumor volume when the treatment was initiated). For historical evaluation, mice were sacrificed by overdosed CO_2 and cervical dislocation after the treatment. Tumors and organs were collected and fixed with 4% formalin. The slices were stained with hematoxylin and eosin and images were collected using a Nikon Eclipse E600 microscope.

1. Vogel, A. & Venugopalan, V. Mechanisms of pulsed laser ablation of biological tissues. *Chem. Rev.* **103**, 577–644 (2003).
2. Fiedler, V. U. *et al.* Laser-induced interstitial thermotherapy of liver metastases in an interventional 0.5 tesla MRI system: Technique and first clinical experiences. *J. Magn. Reson. Imaging* **13**, 729–737 (2001).
3. Shao, J. *et al.* Photothermal nanodrugs: potential of TNF-gold nanospheres for cancer theranostics. *Sci. Rep.* **3**, 1293 (2013).
4. Yang, K. *et al.* Multimodal imaging guided photothermal therapy using functionalized graphene nanosheets anchored with magnetic nanoparticles. *Adv. Mater.* **24**, 1868–1872 (2012).
5. Yu, M. K. *et al.* Image-guided prostate cancer therapy using aptamer-functionalized thermally cross-linked superparamagnetic iron oxide nanoparticles. *Small* **7**, 2241–2249 (2011).
6. Peng, C. L. *et al.* Multimodal image-guided photothermal therapy mediated by 188Re-labeled micelles containing a cyanine-type photosensitizer. *ACS Nano* **5**, 5594–5607 (2011).
7. Bardhan, R., Lal, S., Joshi, A. & Halas, N. J. Theranostic nanoshells: from probe design to imaging and treatment of cancer. *Acc. Chem. Res.* **44**, 936–946 (2011).
8. Goldberg, B. B., Liu, J. B. & Forsberg, F. Ultrasound contrast agents: a review. *Ultrasound Med. Biol.* **20**, 319–333 (1994).
9. Calliada, F., Campani, R., Bottinelli, O., Bozzini, A. & Sommaruga, M. G. Ultrasound contrast agents: basic principles. *Eur. J. Radiol.* **27** Suppl 2, S157–160 (1998).
10. Cosgrove, D. Ultrasound contrast agents: an overview. *Eur. J. Radiol.* **60**, 324–330 (2006).
11. Baac, H. W. *et al.* Carbon-nanotube optoacoustic lens for focused ultrasound generation and high-precision targeted therapy. *Sci. Rep.* **2**, 989 (2012).
12. Sandhu, I. S. & Bhutani, M. S. Gastrointestinal endoscopic ultrasonography. *Med. Clin. North. Am.* **86**, 1289–1317 vi (2002).
13. Seip, R. & Ebbini, E. S. Noninvasive Estimation of Tissue Temperature Response to Heating Fields Using Diagnostic Ultrasound. *Ieee. T. Bio-Med. Eng.* **42**, 828–839 (1995).
14. Varghese, T. *et al.* Ultrasound monitoring of temperature change during radiofrequency ablation: Preliminary in-vivo results. *Ultrasound Med. Biol.* **28**, 321–329 (2002).
15. Ke, H. T. *et al.* Gold-Nanoshelled Microcapsules: A Theranostic Agent for Ultrasound Contrast Imaging and Photothermal Therapy. *Angew. Chem. Int. Edit.* **50**, 3017–3021 (2011).
16. Ke, H. *et al.* Bifunctional gold nanorod-loaded polymeric microcapsules for both contrast-enhanced ultrasound imaging and photothermal therapy. *J. Mater. Chem.* **21**, 5561–5564 (2011).
17. Zha, Z. *et al.* Targeted delivery of CuS nanoparticles through ultrasound image-guided microbubble destruction for efficient photothermal therapy. *Nanoscale,* DOI: 10.1039/C1033NR00541K (2013).
18. Sharifi, S. *et al.* Toxicity of nanomaterials. *Chem. Soc. Rev.* **41**, 2323–2343 (2012).
19. Ghosh, P., Han, G., De, M., Kim, C. K. & Rotello, V. M. Gold nanoparticles in delivery applications. *Adv. Drug Deliv. Rev.* **60**, 1307–1315 (2008).
20. Nel, A., Xia, T., Madler, L. & Li, N. Toxic potential of materials at the nanolevel. *Science* **311**, 622–627 (2006).
21. Shen, Y. *et al.* Prodrugs forming high drug loading multifunctional nanocapsules for intracellular cancer drug delivery. *J. Am. Chem. Soc.* **132**, 4259–4265 (2010).
22. Ma, Y., Dai, Z., Zha, Z., Gao, Y. & Yue, X. Selective antileukemia effect of stabilized nanohybrid vesicles based on cholesteryl succinyl silane. *Biomaterials* **32**, 9300–9307 (2011).
23. Jang, J. & Yoon, H. Multigram-scale fabrication of monodisperse conducting polymer and magnetic carbon nanoparticles. *Small* **1**, 1195–1199 (2005).
24. Hong, J. Y., Yoon, H. & Jang, J. Kinetic study of the formation of polypyrrole nanoparticles in water-soluble polymer/metal cation systems: a light-scattering analysis. *Small* **6**, 679–686 (2010).
25. Oh, W. K., Yoon, H. & Jang, J. Size control of magnetic carbon nanoparticles for drug delivery. *Biomaterials* **31**, 1342–1348 (2010).
26. Ramanaviciene, A., Kausaite, A., Tautkus, S. & Ramanavicius, A. Biocompatibility of polypyrrole particles: an in-vivo study in mice. *J. Pharm. Pharmacol.* **59**, 311–315 (2007).
27. Au, K. M., Lu, Z., Matcher, S. J. & Armes, S. P. Polypyrrole nanoparticles: a potential optical coherence tomography contrast agent for cancer imaging. *Adv. Mater.* **23**, 5792–5795 (2011).
28. Zha, Z., Yue, X., Ren, Q. & Dai, Z. Uniform polypyrrole nanoparticles with high photothermal conversion efficiency for photothermal ablation of cancer cells. *Adv. Mater.* **25**, 777–782 (2013).
29. Bai, M. Y., Cheng, Y. J., Wickline, S. A. & Xia, Y. Colloidal hollow spheres of conducting polymers with smooth surface and uniform, controllable sizes. *Small* **5**, 1747–1752 (2009).
30. Jang, K. S., Ko, H. C., Moon, B. & Lee, H. Observation of photoluminescence in polypyrrole micelles. *Synthetic Met.* **150**, 127–131 (2005).
31. Oh, E. J., Jang, K. S. & MacDiarmid, A. G. High molecular weight soluble polypyrrole. *Synthetic Met.* **125**, 267–272 (2001).
32. Lin, H. *et al.* Conducting polymer composite film incorporated with aligned carbon nanotubes for transparent, flexible and efficient supercapacitor. *Sci. Rep.* **3**, 1353 (2013).
33. Bae, W. J., Kim, K. H., Park, Y. H. & Jo, W. H. A novel water-soluble and self-doped conducting polyaniline graft copolymer. *Chem. Commun. (Camb),* 2768–2769 (2003).
34. Neuberger, T., Schopf, B., Hofmann, H., Hofmann, M. & von Rechenberg, B. Superparamagnetic nanoparticles for biomedical applications: Possibilities and limitations of a new drug delivery system. *J. Magn. Magn. Mater.* **293**, 483–496 (2005).

Acknowledgments

This work was financially supported by National Natural Science Foundation for Distinguished Young Scholars (No. 81225011), State Key Program of National Natural Science of China (Grant No. 81230036).

Author contributions

Z.B. Zha and Z.F. Dai conceived the project, interpreted the data and wrote the manuscript. Z.B. Zha and S.H. Zhang prepared the PPyHMs starting materials and carried out the *in vitro* characterization. J.R. Wang, S.M. Wang, E.Z. Qu and Y.S. Jin carried out the ultrasound imaging experiment. Z.B. Zha and S.M. Wang carried out the *in vivo* photothermal tumor ablation. Z.B. Zha and E.Z. Qu carried out the historical evaluation experiment. All authors reviewed the manuscript.

Additional information

Supplementary information accompanies this paper at http://www.nature.com/scientificreports

Competing financial interests: The authors declare no competing financial interests.

How to cite this article: Zha, Z.B. *et al.* Polypyrrole Hollow Microspheres as Echogenic Photothermal Agent for Ultrasound Imaging Guided Tumor Ablation. *Sci. Rep.* **3**, 2360; DOI:10.1038/srep02360 (2013).